

# Fracture behaviors of cementitious materials and renewed RC box culverts

S.Ishiguro

*Faculty of Bioresources, Mie University, Tsu, Japan*

M.Ishii & T.Nonaka

*Faculty of Life and Environmental Science, Shimane University, Matsue, Japan.*

H.Nakagawa

*Piping Products & Systems Development Center, Sekisui Chemical Co., LTD., Kyoto, Japan*

**ABSTRACT:** Material experiments for the polymer cement mortar and concrete are performed to evaluate the mechanical properties. The fracture mechanical parameters such as the specific fracture energy and tension softening diagram are analyzed from the load-displacement curves measured using rectangular notched specimens and wedge-splitting procedures. Using these data, numerical nonlinear analyses are carried out to investigate the fracture behaviors of a composite pipe renewed by the SPR (Spirally Pipe Renewal) method under internal water pressure conditions. The results are compared with experimental results, and the reliability of the analyses is examined. It is concluded that the resistance against internal water pressure can be improved with this renewal method.

**Keywords:** Polymer cement mortar, Fracture energy, Tension softening, Composite pipe, Fracture analysis

## 1 INTRODUCTION

Many of the RC culverts used as irrigation, drainage, and sewage channels have been damaged and are in need of repair or renewal. The SPR (Spirally Pipe Renewal) method is expected to be effective in renewing these damaged culverts. However, the procedures of the design and performance verification have not been determined, and the analytical method to evaluate the stiffness and strength of renewed pipe must be developed.

In this study, material experiments are conducted to evaluate the mechanical properties of polymer cement mortars used for the repair or renewal works. Fracture parameters of the materials as well as the strengths are very important for the analyses and examination of the structural behaviors of renewed pipes. Therefore, the experiments and analyses are focused on the evaluation of fracture properties of the polymer cement mortars, which are newly developed for SPR methods. Fracture mechanical parameters such as the specific fracture energy, the notch tensile strength and the tension softening diagram are analyzed from the load-displacement curves measured by rectangular notched specimens and wedge-splitting procedures.

Using these data, numerical nonlinear analyses

are carried out to investigate the fracture behaviors of an SPR composite pipe under internal water pressure conditions. The results are compared with experimental results, and the reliability of the analyses is examined and discussed.

## 2 MATERIAL EXPERIMENTS

### 2.1 Basic properties of materials

Two kinds of polymer cement mortar (MA and MB) with siliceous sand and light-weight fine aggregate were tested. The mix ratio, compressive, tensile and bending strengths, modulus of elasticity, ultimate compressive strain ( $\epsilon_{cu}$ ) are listed in Table 1 for MA and MB mortar. In the mixtures ordinary Portland cement and polyacrylic acid ester emulsion are used as a binder.

The specimens were allowed to harden for 24 hours after casting, before being removed from their molds and cured in water for 3 days. After the curing in water, the specimens were wrapped in a thin plastic sheet and stored in a chamber at a temperature of 23 °C until testing.

The mortar specimens were tested under the different ages of 7, 28 and 91 days. All testings were performed on three identical specimens of each

Table 1. Properties of polymer cement mortar

		MA-mortar	MB-mortar
W/C (%)		41	60
P/C (%)		6.3	8.3
Type of aggregate		Siliceous sand	Light-weight fine aggregate
Type of polymeric admixture		PAE	PAE
Unit weight (g/cm <sup>3</sup> )		2.15	1.60
$f_c$ (MPa)	Age (day)		
	7	43.6	24.5
	28	51.2	28.6
$f_t$ (MPa)	7	4.47	2.11
	28	4.58	2.31
	91	4.84	2.72
$f_b$ (MPa)	7	9.65	5.80
	28	10.8	6.65
	91	11.0	7.54
$E_c$ (GPa)	7	22.6	7.59
	28	22.1	8.76
	91	23.8	10.4
$cu$	28	0.0028	0.0038

material to obtain sufficient data for a statistical evaluation. The bending strength  $f_b$  and compressive strength  $f_c$  are obtained from the tests using a bending specimen of 40mm × 40mm × 160mm. The tensile strength  $f_t$  is determined from the cylindrical specimen with 75 mm height and 50 mm diameter. The modulus of elasticity  $E_c$  is estimated from the compressive stress-strain relation measured by the cylindrical specimen with 100 mm height and 50 mm diameter, and a 30 mm wire strain gauge.

In order to characterize the mechanical properties of mortar compared to concrete, a normal strength concrete (CA) was also tested and investigated using the cylindrical specimen with 200 mm height and 100 mm diameter. The test results at an age of 28 days are listed in Table 2.

Table 2. Properties of concrete

	CA-concrete
Cement (kg/m <sup>3</sup> )	336
Water (kg/m <sup>3</sup> )	168
Water cement ratio W/C (%)	50
Type of coarse aggregate	River gravel
Maximum size of aggregate $G_{max}$ (mm)	20
$f_c$ (MPa)	32.2
$f_t$ (MPa)	2.72
$E_c$ (GPa)	26.1

## 2.2 Fracture testing method

A schematic of the wedge-splitting test method, originally developed by Tschegg et al. (1991, 1995), is given in Figure 1. The single-edge notched specimen is placed on a narrow linear support in a compression-testing machine. A wedge-splitting apparatus, comprised of a wedge and load transmission pieces, is placed into a groove (see Figure 1(a)). The wedge, starter notch, and linear support are vertically aligned, which allows the load to be transmitted directly from the testing machine to the specimen without producing additional lateral loads or moments.

The wedge transmits a force ( $F_m$ ) from the testing machine to the specimen. This force is transformed by the slender wedge into a large horizontal component ( $F_h$ ) and a small vertical component ( $F_v$ ), which are then applied to the specimen (see Figure 1(b)). The large horizontal component splits the specimen in a manner similar to a bending test. A load cell in the testing machine measures the total force ( $F_m$ ). Since the wedge angle ( $\alpha$ ) is known, the

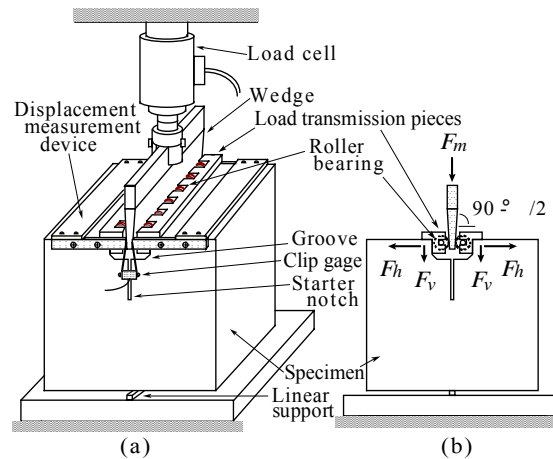


Figure 1. Sketch of wedge-splitting test method and loading arrangements

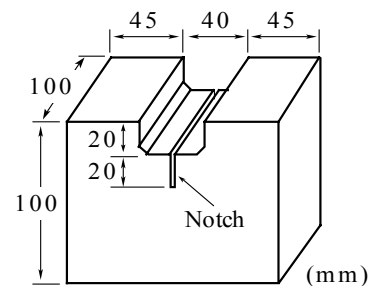


Figure 2. Size and shape of specimen used for fracture test

horizontal component ( $F_h$ ) is calculated as follows.

$$F_h = \frac{F_m}{2 \tan(\alpha/2)} \quad (1)$$

The displacement ( ) of the specimen, referred to as the Crack Mouth Opening Displacement ( $CMOD$ ), is measured at each end of the groove using a clip gauge. The mean values of the two measurements are used to reduce the uncertainty. Tests were performed using a mechanical compression-testing machine with a load capacity of 9.8 kN. The crosshead velocity for each test was 0.67 mm/min.

A rectangular notched specimen, illustrated in Figure 2, was used for fracture tests of the mortars (MA, MB) and concrete (CA). A starter notch (2 mm wide) was cut in the top of the specimen with a stone saw shortly before testing. The ligament length is 60 mm for all specimens.

### 2.3 Load-displacement diagram

The force ( $F_m$ ) and the two end displacements ( 1 and 2) were recorded by an electronic data logger at 1.0-second intervals. The data were then analyzed to produce a load-displacement curve ( $F_h$ - $CMOD$  curve).

The measured load-displacement curves are given in Figures 3 (a) ~ (c) for MA, MB and CA at the different ages. The load-displacement graphs represent the average curve of the three identical specimens at each material age. The scattering of the measured data in the three specimens at each age was small especially in the mortar specimens. Large differences between the MA and MB mortar were observed in the maximum load and the critical  $CMOD$  as plotted in Figures 3(a) and (b). The results also show that the maximum load increased slightly with the increasing material age.

Unstable crack propagation was not observed in the fracture test for mortar and concrete specimens. The wedge-splitting procedures employed for a fracture test method is appropriate to determine the load-displacement curves of the polymer cement mortars and concretes with stable crack propagation until total separation of the materials.

## 3 ANALYSIS OF FRACTURE PARAMETER

The load-displacement graphs indicated in Figures 3 (a) ~ (c) characterize the fracture properties of the mortars and concrete. In this study, the fracture mechanical parameters, such as the specific fracture energy ( $G_f$ ), the notch tensile strength ( $f_{bt}$ ), and the tension softening diagram, are derived from the experimental results.

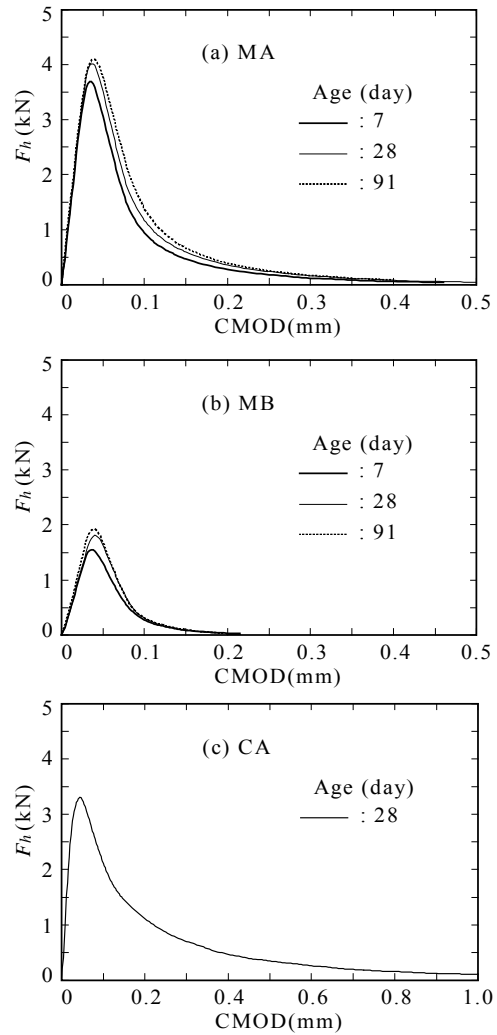


Figure 3. Measured load ( $F_h$ )-displacement ( $CMOD$ ) curves for mortars and concrete at different ages

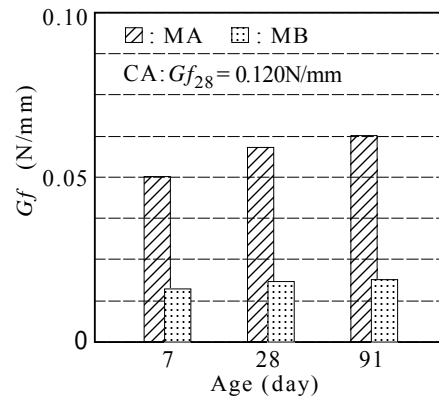


Figure 4. Specific fracture energy  $G_f$  for MA and MB mortar at different ages

### 3.1 Specific fracture energy

The area under the load-displacement curve represents the energy needed to fracture the specimen (fracture energy). The specific fracture energy ( $G_f$ ) is a measure of the crack growth resistance of the material and is defined as the ratio of fracture energy to fracture area, normal to the wedge penetration direction.

The specific fracture energy ( $G_f$ ) of the mortar specimens is determined from the test results and is given in Figure 4. The  $G_f$  value of the MA mortar is 0.057 N/mm at the age of 28 days and is almost half of that of the CA concrete (0.12 N/mm). This means that the crack growth resistance of the MA mortar is only half of that of the CA concrete. The tensile strength of the MA mortar is higher than that of the CA concrete, as seen from Table 1. These may lead to a brittle failure in mortar specimens, because of the low fracture energy and the low crack growth resistance. On the other hand, the CA concrete with natural gravel shows in high  $G_f$  value due to the higher aggregate interlock compared with the MA mortar. This result was proved by fractographic observations, which show that the fracture surfaces of MA specimens are flatter and less tortuous than those of CA specimens.

The  $G_f$  value of the MB mortar is one third of that of the MA mortar as seen from Figure 4. This means that the specific fracture energy of the polymer cement mortar reacts sensitively to changes of the fine aggregate as well as the mix proportions. The low  $G_f$  value in the MB mortar probably resulted from the lower aggregate interlock during crack propagation in comparison with the MA mortar.

Comparing the mechanical properties of MA mortar for the age of 28 days to that of MB mortar yields the following values:

$$\begin{aligned} f_c(\text{MB}) / f_c(\text{MA}) &= 0.56, & f_t(\text{MB}) / f_t(\text{MA}) &= 0.51 \\ f_b(\text{MB}) / f_b(\text{MA}) &= 0.62, & G_f(\text{MB}) / G_f(\text{MA}) &= 0.31 \end{aligned}$$

These results show that the  $G_f$  values are lowest in comparison with the other mechanical properties. The light-weight fine aggregate used in the MB mortar does not lead to as high fracture resistances as does the siliceous sand.

### 3.2 Notch tensile strength

The maximum load in the load-displacement diagram ( $F_{lmax}$ ) may be used to calculate the conventional notch tensile strength ( $f_{bt}$ ), as described by Tschegg et al. (1995). The notch tensile strength is calculated as follows:

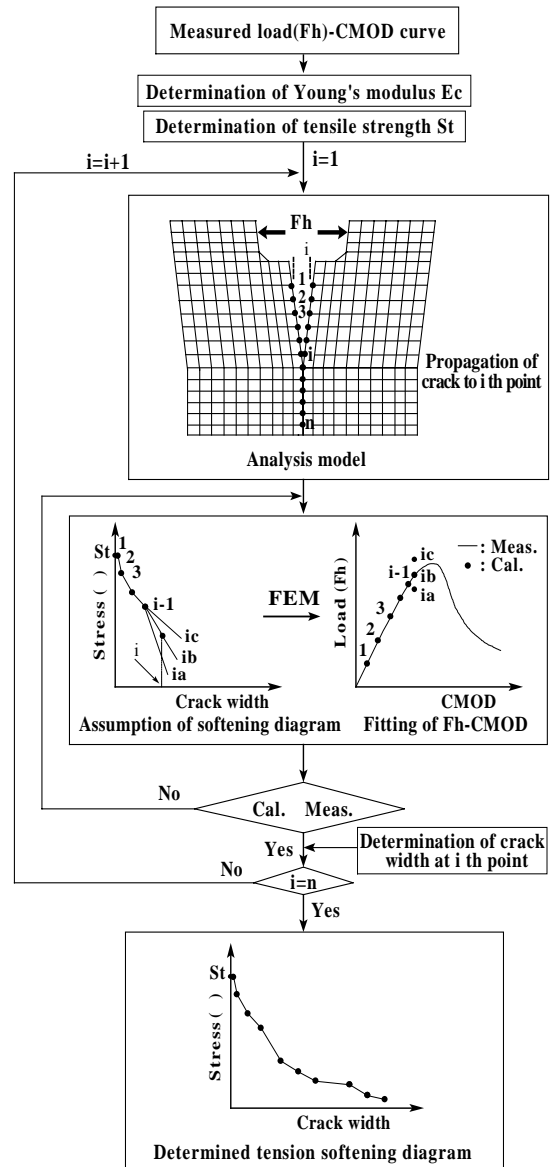


Figure 5. Flow diagram of polylinear inverse analysis method

Table 3. Calculated notch tensile strength ( $f_{bt}$ )

	Age (day)	MA	MB	CA
$f_{bt}$ (MPa)	7	4.67	1.96	-
	28	5.09	2.31	4.19
	91	5.19	2.44	-

$$f_{bt} = \frac{M}{W_{lig}} + \frac{F_{h\max}}{A_{lig}} \quad (2)$$

$$M = y \cdot F_{h\max} \quad (3)$$

$$W_{lig} = \frac{B_{lig} \cdot H_{lig}^2}{6} \quad (4)$$

$$A_{lig} = B_{lig} \cdot H_{lig} \quad (5)$$

where  $M$  is the maximum moment,  $y$  is the distance from the axis of the force application to the center of the ligament area,  $W_{lig}$  is the maximum moment of resistance, referred to as the notch root, and  $A_{lig}$  is the area of the plane projection of the ligament area.

The calculated notch tensile strengths are listed in Table 3 for the MA and MB mortars. The notch tensile strengths of the mortars for ages up to 91 days slightly increased, and the behaviors were similar to those of the tensile strengths or bending strengths determined by the material experiments. The results also show that the  $f_{bt}$  value is lower than the  $f_b$  value for the mortars and is similar to the  $f_t$  value. The notch tensile strength calculated from the wedge-splitting test results serves as a fracture mechanical parameter for the newly developed materials.

### 3.3 Tension softening diagram

In order to characterize the fracture behavior of mortars fully, the strain softening behavior must be determined from a tension softening diagram. The tension softening diagram characterizes the relation between the crack width and the tensile stress of the materials and is useful for evaluating the toughness of new materials and fiber-reinforced concrete. The evaluation methods of the tension softening diagram are classified into some groups (Mihashi et al. 2001). In this study, a polylinear inverse analysis was used to determine the exact shape of the tension softening diagram from the measured load-displacement curves.

The polylinear inverse analysis was based on the finite element method applied using the fictitious crack model (Uchida et al. 1995), and was developed specifically for the wedge-splitting loading conditions (Ishiguro, 2001). A flow diagram of the polylinear inverse analysis method is provided in Figure 5. Details may be found in (Kitsutaka et al. 2001).

The characteristic values of the polylinear softening diagram are obtained using an iterative best-fit procedure to match the calculated and measured load ( $F_h$ )-displacement ( $CMOD$ ) curves. A  $F_{hcal}/F_{hmeas}$  ratio between 0.999 and 1.001 ( $\pm 0.1\%$ ) was used as the tolerance for the fitting

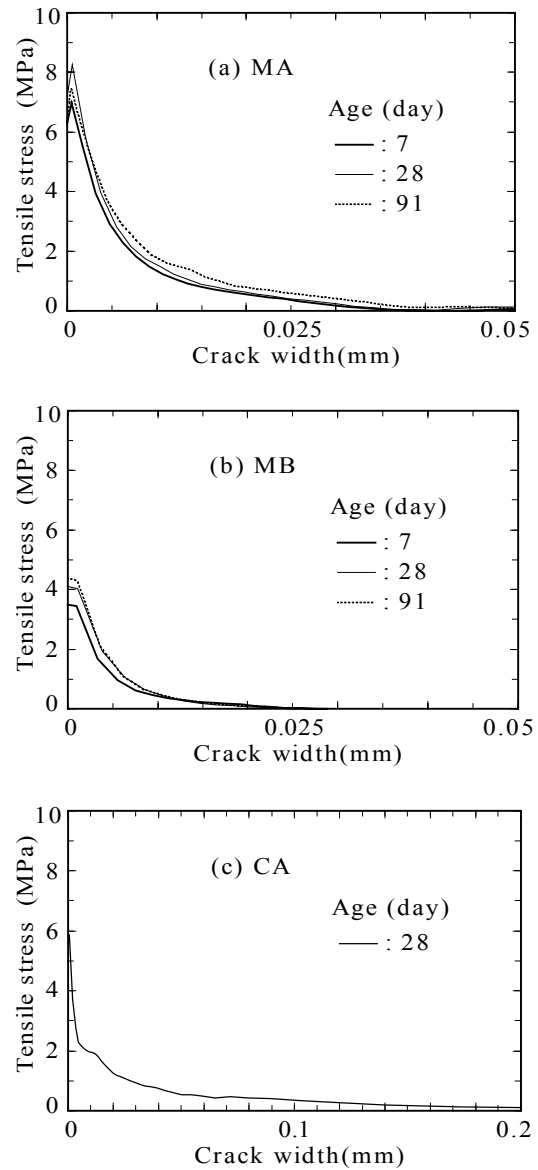


Figure 6. Determined tension softening diagrams for polymer cement mortars (MA and MB) and concrete (CA)

procedure.

The calculated tension softening diagrams for MA, MB and CA are given in Figures 6 (a) ~ (c) for the different ages of 7, 28 and 91 days. The results show that the critical crack width is approximately 0.05 mm and 0.025 mm for the MA and MB mortar respectively. The values are far smaller than that of the CA concrete (more than 0.20 mm). This shows that the mortars have the lower aggregate interlock during crack propagation. The diagrams also show that the cohesive stress at the lower part of the

Table 4. Young's modulus ( $E_c$ ) and tensile strength ( $S_t$ ) determined by inverse analysis

	Age (day)	MA	MB	CA
$E_c$ (GPa)	7	23.8	8.30	-
	28	24.0	8.52	22.4
	91	24.6	9.45	-
$S_t$ (MPa)	7	6.30	3.50	-
	28	7.20	4.10	5.80
	91	6.20	4.35	-

post-peak curve is higher for the concrete than for the mortars. Thus, the higher cohesive stress at the lower part of the curve is induced as a result of an aggregate interlock, which leads to an increase in the fracture energy of the CA concrete.

Young's modulus ( $E_c$ ) and tensile strengths ( $S_t$ ) determined by the analyses are listed in Table 4. The results indicate that the calculated values in  $E_c$  agreed well with the measured ones for the MA and MB mortar. The tensile strengths ( $S_t$ ) at each age, as calculated using the iterative best-fit procedure, were larger than the measured tensile strengths ( $f_t$ ) for the MA and MB mortars.

From the analytical results shown in this section, it is concluded that the polylinear inverse analysis method can provide the required tension softening diagrams from the wedge-splitting test results.

## 4 FRACTURE ANALYSIS OF RENEWED RC BOX CULVERT

### 4.1 Outline of SPR method

The SPR Method was originally developed to renew damaged sewage pipes (Nonaka et al. 2002). As shown in Figures 7 and 8, an inner pipe is formed by coiling a strip called profile, which consists of vinyl chloride and steel reinforcement. The gap between the existing and inner pipes is filled with the polymer cement mortar to bond them together and make a composite pipe.

The vinyl chloride surface provides durability against physical, chemical and biological erosion, so this method is quite effective for the renewal of sewage pipes. At the same time, its smoothness as opposed to concrete provides an equivalent flow rate to the renewed pipe, whose diameter is smaller than the original pipe. This method can renew damaged or old pipes without the reduction of their

maximum flow rate.

The mechanical strength of a renewed pipe is provided by the composite structure of the old pipe, filling mortar, and reinforcement of the profile. Therefore, their bonding is quite important, as well as their individual strength. It is possible to achieve the same or better strength compared to the original pipe against internal water pressure, external earth pressure, and earthquake stress.

### 4.2 Model experiment

A model experiment was conducted based on the geometry and materials, using the specimen shown in Figure 9. The thickness of the specimen is 1 m. Rubber gaskets and steel plates were attached to a renewed culvert, to apply and keep internal water pressure (see Figure 10). Initial pressure of 0.092 MPa was applied and kept for 7 days, and no leakage or decrease of pressure was observed.

After that, the pressure was increased with a 0.01 MPa step and kept for 30 seconds and 5 minutes. The limit of the pressure was determined as 0.21 MPa, based on the results of the analyses. At every

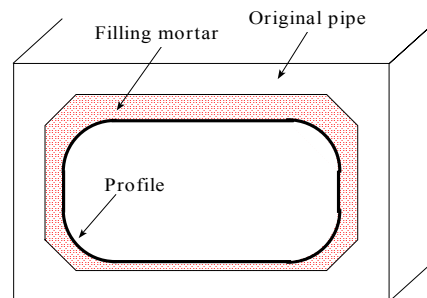


Figure 7. Schematic view of SPR composite pipe



Figure 8. Installation of inner pipe with profile

stage of the pressure, cracks and leakages are inspected visually. At 0.2 MPa, a longitudinal cracking occurred in the middle of the lower slab. Moreover, its growth and latitudinal cracks in the upper slab were observed at 0.21 MPa.

During the experiment, strain was measured using strain gauges attached to the specimen. However, significant strain could not be measured except for the gauge crossing the crack. Details of the experiments and analyses have been reported by (Ishii et al. 2003).

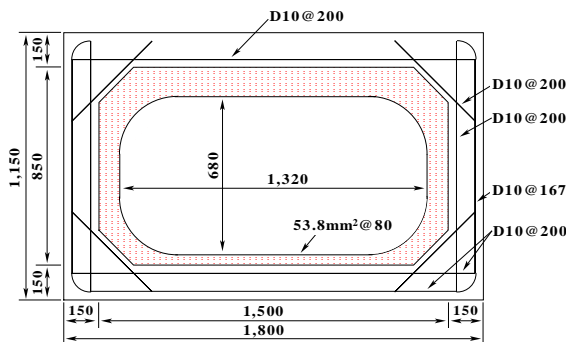


Figure 9. Dimensions and reinforcements of the specimen



Figure 10. Set-up for internal water pressure tests

Table 5. Mechanical properties of concrete and filling mortar used for FEM analysis

	$f_c$ (MPa)	$f_t$ (MPa)	$E_c$ (GPa)	$G_f$ (N/mm)
Concrete*	40.5	2.71	31.1	0.151
Filling mortar**	41.7	3.72	21.2	0.055

\* W/C=40%,  $G_{max}=25$  mm, \*\* Polymer cement mortar: MA

### 4.3 Nonlinear FEM analysis

Fracture analyses are carried out using commercial software (ATENA, 2003). It was developed for fracture analyses of RC structures and possesses several constitutive models for concrete and reinforcement. The mechanical properties used in the constitutive model, such as compressive and tensile strengths, ultimate strain, Young's modulus, can be set separately. The constitutive model of concrete is applied for the concrete and filling mortar, and all of the material properties listed in Table 5 are used in the analyses. The tension softening diagrams are expressed by an exponential function for the filling mortar and concrete, based on the results of the inverse analyses.

The constitutive model of steel that considered yielding is used for the reinforcements of the culvert and profile. Young's moduli ( $E_s$ ) and yielding stresses ( $f_y$ ) are set as follows based on their specified values.

Reinforcement of culvert:  $E_s=200$ GPa,  $f_y=295$ MPa.  
Profile reinforcement :  $E_s=170$ GPa,  $f_y=210$ MPa.

Loads considered in the analyses are weight and internal water pressure. Weight of the whole structure is applied as a distributed force throughout the analyses. The water pressure is increased in a step-by-step manner, analyzing and checking the situation of the structure at every pressure stage.

This culvert is placed on steel H-beams in the experiment, so the simple support used in the analyses is in accordance with the experimental conditions.

The distributions of deformation, stress, strain and cracks are obtained for every stage of internal water pressure. Among them, the positions of cracks and the water pressure at their occurrences are summarized as follows. The lower slab, which has the thinnest filling layer, leads to cracking on its outer side of the culvert with the smallest water pressure, 0.17 MPa.

Cracking of the upper slab occurs with the pressure of 0.25 MPa, owing to its thick filling layer. The progress of cracks in the culvert is not significant up to 0.28 MPa, but rapid growth is observed at 0.29MPa, as shown in Figures 11(a) and (b). With 0.29 MPa of internal pressure, deep cracks on the lower part of side walls approaching the inner reinforcement, and large deformation occurs. Though the resistance against internal water pressure still remains after the fracture, this situation, which can lead to a brittle failure, should be averted.

To examine the efficiency of the enhancement, similar analyses are conducted for the original culvert. The first occurrence of cracking is expected

at the inner side of side walls near haunches, with the pressure of 0.06 MPa. In the renewed case, this portion is covered with filling mortar, and the cracking at the surface of the mortar does not occur until 0.28 MPa because of its strength and profile reinforcement. The ultimate calculated resistance against internal pressure is 0.11 MPa, less than half that of composite pipes. The SPR method is able to enhance the resistance of RC culverts against internal pressure, and can be used for their conversion to pipelines.

Detailed comparison of the stress and strain between the analytical and experimental results could not be executed, but it was concluded that the results of the analyses were accurate and close to the result of the experiment. Therefore, the analysis based on accurate material properties is reliable so that it can be used for the performance verification of structures.

## 5 CONCLUSIONS

Fracture mechanical parameters of polymer cement

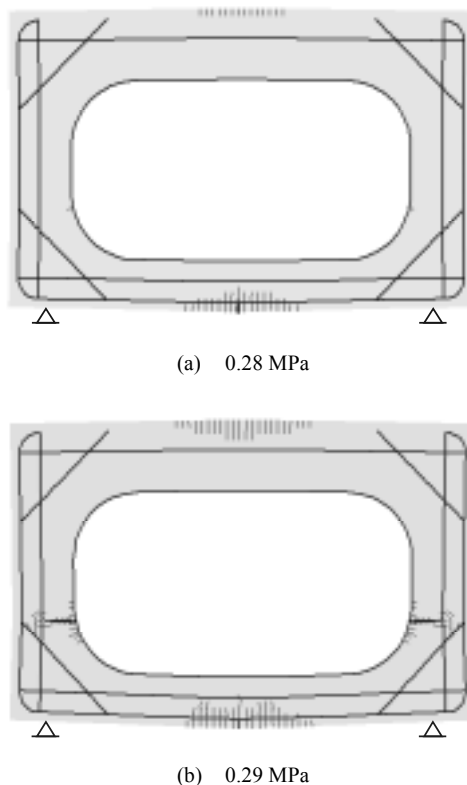


Figure 11. Analytical results of crack growth in a renewed RC box culvert subjected to internal water pressure

mortars were determined with wedge-splitting and the polylinear inverse analysis method. Using these data, numerical analyses have been performed to investigate the fracture behaviors of SPR composite pipes. The results were summarized as follows:

1. The wedge-splitting test method is appropriate to obtain a stable load-displacement curve for the polymer cement mortars and concretes.
2. The polylinear inverse analysis method is very useful to determine the required tension softening diagrams from the wedge-splitting test results.
3. The specific fracture energy of the polymer cement mortar is far smaller than that of the concrete, and brittleness under tension is observed.
4. Model experiments and numerical analyses were conducted for SPR composite pipes subjected to internal water pressure.
5. The experimental and analytical results indicated that the resistance against internal water pressure could be improved with the renewal method.

## REFERENCES

- ATENA 2003, Computer Program, Ver2.1.8, Praha, Cervenca Consulting.
- Ishiguro, S. 2001. Softening properties of concrete under biaxial loading. In R.D. Borst, J. Mazars, G. P. Cabot & J. G. M. van Mier (eds.), *Proc. of the 4th Int. Conf. on Fracture Mechanics of Concrete Structures* Lisse, BALKEMA: 357-362.
- Ishii, M., Nonaka, T., Ishiguro, S. & Nakagawa, H. 2003. Fracture experiments and analyses of renewed RC box culvert. In K.S. Yeon (ed.), *Proc. of the 4th Asia Symposium on Polymers in Concrete, Chuncheon, Korea*: 285-292.
- Kitsutaka, Y., Uchida, Y., Mihashi, H., Kaneko, Y. & Nakamura, N., Kurihara, N. 2001. Draft on the JCI standard test method for determining tension softening properties of concrete. In R.D. Borst, J. Mazars, G. P. Cabot & J. G. M. van Mier (eds.), *Proc. of the 4th Int. Conf. on Fracture Mechanics of Concrete Structures* Lisse, BALKEMA: 371-376.
- Mihashi, H., Kaneko, Y., Kirikoshi, K., Otsuka, K. & Akita, H. 2001. Test methods for determining tension softening diagram for concrete. In R.D. Borst, J. Mazars, G. P. Cabot & J. G. M. van Mier (eds.), *Proc. of the 4th Int. Conf. on Fracture Mechanics of Concrete Structures* Lisse, BALKEMA: 403-411.
- Nonaka, T., Ishii, M., Ishiguro, S. & Maeda, H. 2002. Renovation methods for agricultural pipe-line facilities, *Journal of JSIDRE*, 70: 1103-1107 (in Japanese).
- Tschegg, E.K. 1991. New equipment for fracture tests on concrete. *Material Testing*, 33: 338-343.
- Tschegg, E.K., Elser, M. & Tschegg-Stanzl, S.E. 1995. Biaxial fracture tests on concrete – development and experience. *Cement and Concrete Composites*, 17: 57-75.
- Uchida, Y., Kurihara, N., Rokugo, K. & Koyanagi, W. 1995. Determination of tension softening diagrams of various kinds of concrete by means of numerical analysis. In F.H. Wittmann (ed.), *Proc. of the 2nd Int. Conf. on Fracture Mechanics of Concrete Structures*, Freiburg, Aedificatio: 17-30.